

An experimental study of wound healing after applying a gelatin-  
based hydrogel sheet to the resected part of rat submandibular gland

Yusuke Miyake

Nihon University Graduate School of Dentistry

Major in Oral and Maxillofacial Surgery

(Directors: Prof. Morio Tonogi, Associate Prof. Osamu Shimizu)

## Index

Abstract	-----	2
Introduction	-----	3
Materials and Methods	-----	4
Results	-----	5
Discussion	-----	7
Conclusions	-----	10
Acknowledgements	-----	10
References	-----	11
Figures	-----	13

This thesis is based on the following article with additional data on proliferating cell nuclear antigen (PCNA) examined immunohistologically:

Yusuke Miyake, Osamu Shimizu, Hiroshi Shiratsuchi, Takaaki Tamagawa, and Morio Tonogi  
Wound healing after applying a gelatin-based hydrogel sheet to resected rat submandibular gland. *Journal of Oral Science*. in press.

## **Abstract**

The present study was performed to prepare a useful experimental model for analysis of the effects of physiologically active substances on the atrophy and regeneration of salivary gland acinar cells. Resection wounds (3-mm diameter) were made in the submandibular glands of 8-week-old Wistar rats ( $n = 24$ ) for histochemical examination on Days 3, 5, 7, 10, 14, and 21 after implantation of the gelatin-based hydrogel sheet. Cell proliferation was assessed immunohistochemically by examining proliferating cell nuclear antigen (PCNA) staining. The results showed that the sheet disappeared nearly by Day 10. Regions around the resection wounds were classified as normal, atrophic, or necrotic. In atrophic regions, acinar cells began to atrophy after resection and the smallest number of acinar cells were observed on Day 7. On Days 5 and 7, striated and granular ducts were observed as duct-like structures. On Day 10, newly formed acinar cells were observed with increased periodic acid-Schiff staining; thereafter, mature acinar cells have increased. In necrotic regions, acinar and ductal cells were destroyed, and the acinar cells were enucleated on Day 3; newly formed acinar cells were observed on Day 10. In both the atrophic and necrotic region, large number of PCNA positive cells were observed in the duct-like structures and ductal epithelial cell nests on Day 7. Thus, the experimental model demonstrated the atrophy and regeneration of the submandibular gland, enabling analysis of the sustained-release effects of physiologically active substances contained within an implanted sheet.

## Introduction

Salivary gland tissue can be damaged by various diseases, such as sialadenitis, sialolithiasis, trauma, and radiation therapy, which lead to degeneration, atrophy, and necrosis. Various methods are used to examine these pathological conditions, including surgical resection (1-3), duct ligation (4-6), radiation (7,8), laser irradiation (9,10), and histopathological and immunohistochemical analyses.

Milstein (11) and Hanks et al. (1) have reported that newly formed acinar cells may regenerate from resection margin ducts during regeneration after partial resection of salivary glands. Boshell et al. (2) and Batsakis et al. (12) have described that epithelial cells may proliferate at intercalated ducts in surgical resection model. It has been revealed that acinar cells regenerate through pathways other than proliferation of residual acinar cells by duct ligation model, suggesting that the epithelia of intercalated ducts and duct-like structures (a luminal structure that could not distinguish from the striated, intercalated, or granular ducts) contain cells that can regenerate into acinar cells (13). Furthermore, regeneration of acinar cells around a laser irradiation-induced necrotic wound has been observed in epithelial cell nests of duct-like structures (9,10). However, the mechanisms by which the progenitor cells proliferate and differentiate into acinar cells remain unclear.

Immunohistochemical studies regarding the atrophy and regeneration of the salivary glands in the above experimental systems have revealed the localization of growth factors such as epidermal growth factor (EGF) (14,15), fibroblast growth factors (FGFs) (16), and nerve growth factor (NGF) (14). The experiments such as retrograde infusion of growth factors have been performed (17). However, the experiments are insufficient to search for long-term effects. Tabata et al. (18) recently investigated whether a gelatin-based hydrogel sheet enable sustained-release of physiologically active substances. They found that the gelatin-based hydrogel sheet allowed 1) topical administration of physiologically active substances; 2) stabilization of physiologically active substances that were easily degraded and inactivated *in vivo*; and 3) sustained-release of physiologically active substances for approximately 2 weeks.

Therefore, in the present study, a round resection wound was prepared using a biopsy punch on the rat submandibular gland, into which a sustained-release sheet was implanted. The histology and cell proliferation in the healing glandular tissue was examined to determine the usefulness of this experimental model for analyzing the effects of physiologically active substances on the atrophy and regeneration of acinar cells.

## Materials and Methods

### I. Animals

Twenty-four 8-week-old male Wistar rats (Sankyo Labo Service Corporation, Tokyo, Japan) were used in this study. The rats underwent 1-week adaptation to the environment at the Animal Experimentation Committee of Nihon University School of Dentistry. All procedures were conducted in accordance with the Animal Experiment Guidelines of the Nihon University School of Dentistry (approval number: AP16D045).

### II. Submandibular gland resection model

For general anesthesia, a mixture of three anesthetics consisting of 0.15 mg/kg medetomidine hydrochloride (Nippon Zenyaku Kogyo, Fukushima, Japan), 2 mg/kg midazolam (Sandoz, Yamagata, Japan), and 2.5 mg/kg butorphanol tartrate (Meiji Seika Pharma, Tokyo, Japan) was intraperitoneally administered to each rat, in combination with isoflurane (2% Forane inhalation anesthetic solution, AbbVie, Tokyo, Japan). Before surgery, 0.2ml of 2% lidocaine hydrochloride (Nissin Pharmaceutical, Yamagata, Japan) was applied for local anesthesia in the submandibular region. A 2 cm skin incision was made in the middle of the anterior neck to expose the submandibular gland, followed by pull-through resection of the caudal region in the submandibular gland with 3-mm disposable biopsy punches (Biopsy Trepan; Kai Industries, Gifu, Japan) (Fig. 1A). A gelatin-based hydrogel sheet (MedGel; MedGEL Corporation, Tokyo, Japan) of the same size was implanted into the resected area (Fig. 1B). MedGel comprises cross-linked, water-solubilized gelatin (a gelatin-based hydrogel sheet) that allows sustained-release of a physiologically active substance over 2 weeks according to a product sheet by the manufacturer.

### III. Histochemical observation

Rats were euthanized with carbon dioxide on Day 3, 5, 7, 10, 14 and 21 after surgery, and their submandibular glands were excised. The glands were fixed in 4% paraformaldehyde for 24 h, then embedded in paraffin blocks as described previously (19). The tissues were sliced at 8  $\mu$ m in thickness with a microtome, and stained with hematoxylin and eosin (HE) or periodic acid-Schiff (PAS) staining.

For immunohistochemical analysis, the sections were deparaffinized and incubated with Tris/borate/EDTA-based buffer (pH 8, 98°C) for 40 min to activate the antigen. To block the non-specific binding, the specimens were incubated with 1% bovine serum albumin (BSA)-phosphate-buffered saline (PBS) for 30 min at room temperature (RT). The specimens were incubated with anti-PCNA antibody (x1,000 diluted with 1% BSA-PBS) (PC10, sc-56, 4  $\mu$ g/ml, Santa Cruz Biotechnology, CA, USA) for overnight at 4°C. After wash with PBS, the specimens were incubated with horseradish peroxidase (HRP)-conjugated secondary antibodies (10  $\mu$ g/ml diluted with 1% BSA-PBS) for 60 min at RT. After extensive wash with PBS, the color reaction was performed with 0.42 mg/ml 3,3'-diaminobenzidine tetrahydrochloride (DAB; Sigma Chemical, MO, USA)- 0.3% H<sub>2</sub>O<sub>2</sub> solution for 10 min at RT. Counter staining was performed with hematoxylin for 1 min at RT. The first antibody was replaced with 4  $\mu$ g/ml normal mouse IgG (Santa Cruz Biotechnology) as negative controls.

## Results

### Histological observation

HE staining images of submandibular glands at Days 3, 5, 7, 10, 14, and 21, are shown in Fig. 2Aa-f. The implanted sheet gradually reduced in size, beginning on Day 3 (Fig. 2Aa, b), and had been reduced to approximately one-third of its original size on Day 7. The sheet also became thinner and fibroblast invasion was observed (Fig. 2Ac). By Day 10, the sheet had mostly disappeared, but could be partially recognized (Fig. 2Ad). However, beginning on Day 14, the sheet could not be recognized in any of the rats (Fig. 2Ae, f). Morphologically, areas around the MedGel sustained-release sheet were classified as follows: a cranial region unaffected by resection; a cranial region adjacent to the sheet, which exhibited atrophy and regeneration; and a caudal region adjacent to the sheet, which exhibited necrosis. The positional relationships between these regions and the resection site are depicted in Fig. 2B. HE and PAS staining images of atrophic and necrotic regions on Days 3-21 after surgery are shown in Fig. 3a-f and Fig. 3g-r, respectively.

### Atrophic region

On Day 3 (Fig. 3a, g), slightly atrophic acinar cells were noted, with small vacuoles scattered in the cytoplasm and slight reduction in the number of secretory granules. In addition, some PAS-positive atrophic acinar cells were observed. Growth of granulation tissue was observed along the duct with slightly obscure basal striations. On Day 5 (Fig. 3b, h), terminal acinar cells exhibited further cytoplasm atrophy and deformation; the numbers of PAS-positive cells were also reduced, compared with those on Day 3. Additional growth of granulation tissue was observed surrounding the duct-like structures, which could not be distinguished from striated and granular ducts.

On Day 7 (Fig. 3c, i), the terminal acinar cells were mostly atrophied and had disappeared. PAS staining of acinar cells was reduced, compared with that on Day 5. In the central part of the epithelial nest, squamoid cells with relatively bright cytoplasm were observed. In the ducts, nuclei exhibited slight hematoxylin staining with cytoplasm atrophy and deformation, indicating a duct-like structure. On Day 10 (Fig. 3d, j), PAS-positive newly formed acinar cells were observed at the tip of the duct-like structure. In addition, duct-like structures with a clear lumen were scattered adjacent to undifferentiated acinar cells. On Day 14 (Fig. 3e, k), immature acinar cells were observed alongside mature cells at the tips of intercalated ducts, which were thinner than the duct-like structures observed on Day 10. On Day 21 (Fig. 3f, l), acinar cells were mostly mature with PAS-positive granules, and intercalated ducts with a clear lumen had gradually aligned, forming a relatively distinct leaflet.

### Necrotic region

On Day 3, a necrotic region was observed at the caudal side of each resection site. The caudal side was slightly edematous, thereby obscuring the boundary between the necrotic region and its surrounding region (Fig. 2Aa). Acinar and ductal cells were mostly destroyed, with enucleated acinar cells and scattered degenerated ducts obscuring the morphology (Fig. 3m). On Day 5, the necrotic region had slightly decreased, compared with that on Day 3 (Fig. 2Ab).

The acini further atrophied, compared with their morphology on Day 3, while fibrous connective tissue increased. In addition, epithelial cell nests consisting of squamoid cells appeared with a few duct-like structures that exhibited granules with slight PAS-positive staining (Fig. 3n).

On Day 7, the necrotic region was shrinking (Fig. 2Ac). Compared with Day 5, more epithelial cell nests were present on Day 7 (Fig. 3o). Squamoid cells with relatively bright cytoplasm were observed in the central portions of epithelial cell nests. The nests varied in size and shape (i.e., round to dendritic) and were connected to duct-like structure with a continuous lumen (Fig. 3o). On Day 10, the necrotic region further decreased in size (Fig. 2Ad). The necrotic region contained a large amount of fibrous connective tissue, with a duct-like structure comprising cubic epithelial cells. In addition, immature acinar cells with PAS-positive granules were located adjacent to the duct-like structure (Fig. 3p). On Days 14 and 21, the necrotic region further decreased in size and exhibited granulation tissue (Fig. 2Ae, f). Many duct-like structures were found in the necrotic region; compared with Day 10, there were increased numbers of acinar cells with PAS-positive granules adjacent to the duct-like structures (Fig. 3q, r).

#### Cell proliferation

##### Atrophic region

Based on the HE staining results, Days 3-7 (Fig. 4a-c) comprised the atrophy process and Days 7-21 (Fig. 4c-f) the regeneration process. A few PCNA-positive cells were observed in intercalated ducts on Day 3 (Fig. 4a) and in duct-like structures on Day 5 (Fig. 4b). During atrophy in the acinar cells, PCNA-positive cells gradually decreased from Day 3 to 7 (Fig. 4a-c). On Day 7, duct-like structures were mainly composed of PCNA-positive cells. PCNA-positive staining was observed in most cells of the duct-like structures on Day 7 (Fig. 4c). In contrast, from Day 10 to 21 (Fig. 4d-f), PCNA-positive cells in duct-like structures gradually decreased, compared with Day 7. On Day 10 (Fig. 4d), many of newly formed acinar cells were PCNA-positive. On Days 14 and 21 (Fig. 4d, f), proliferating cells appeared to decrease with the maturation of acinar cell.

##### Necrotic region

On Days 3 and 5 (Fig. 4g, h), there were acinar cells with nuclei during the atrophy, in addition to enucleated acinar cells; PCNA-positive staining was observed in about half of the acinar cells. On Day 5 (Fig. 4h), PCNA-positive cells began to be observed in duct-like structures. On Day 7 (Fig. 4i), many cells in squamoid cell nests were PCNA-positive. The number of PCNA-positive cells in duct-like structures did not change from Day 10 to 21 (Fig. 4j-l). Newly formed acinar cells were PCNA-positive on Days 14 and 21 (Fig. 4k, l).

##### Normal region

The area away from the resection wound showed no histological changes and was assumed as the normal control region. From Days 3 to 21, PCNA-positive acinar cells were rarely observed (Fig. 4m-r).

## Discussion

The objective of the present study was to prepare an experimental model to examine the effects of physiologically active substances that affect the atrophy and regeneration of acinar cells after salivary gland resection. Submandibular gland tissue was resected with a 3-mm biopsy punch, and a sustained-release sheet was implanted to observe morphological changes in gland tissue on Days 3, 5, 7, 10, 14, and 21.

The sustained-release sheet implanted in the resected region gradually reduced in size to approximately one-third of its original size by Day 7, and the mesh structure of the sheet became thinner. By Day 10, the sheet had mostly disappeared, but could be still recognized. However, on Day 14, the sheet could not be recognized in any of the rats. The manufacturer explained that if the sheet were immersed in a physiologically active substance, it could gradually release that substance for 14 days according to a product sheet by the manufacturer. However, in this experimental model, the sheet could be discernible up to Day 10. The sheet could retain active substance up to 10 days.

In the submandibular gland tissue, three morphological regions (normal, atrophic, and necrotic) were observed near the resected region. In the atrophic region, acinar cells were atrophied and reduced in number after resection, with the smallest number of acinar cells on Day 7. On Days 5 and 7, duct-like structures were found to have replaced striated and granular ducts. Beginning on Day 10, terminal acinar cells gradually regenerated and PAS staining increased. In addition to mature acinar cells, immature cells were observed at the tip of the duct-like structures. On Day 21, the atrophic regions appeared similar to normal glandular tissue. Milstein (11) reported thickening and branching of the lining of the main duct in granulation tissue on Day 5 after partial resection of the submandibular gland; this was followed by division of the duct branches and differentiation into acinar cells on Day 7. Hanks et al. (1) reported degeneration and necrosis in the central lobe of the submandibular gland, as well as marked growth of epithelial cells from undeveloped ductal cells from Days 7 to 14 after resection. These findings are consistent with those of the present study, despite the use of different resection methods, suggesting that acinar cells can be regenerated from remaining ducts.

In the present study, a necrotic region due to vascular insufficiency after resection was observed in the caudal region adjacent to the sheet. On Day 3, the acinar and duct cells were mostly destroyed, with enucleated acini and scattered duct-like structures obscuring the histology. On Day 10, newly formed acinar cells appeared, and these gradually increased until Day 21. Takahashi et al. (9) reported regeneration of the necrotic region after YAG laser irradiation and growth from residual duct-like structures around the necrotic region from Days 1 to 3 after irradiation, which rapidly became highly proliferative ducts. Beginning on Day 7, undifferentiated polygonal cells were differentiated into immature acinar cells. On Day 28, immature acinar cells were mixed with mature cells. Compared with the findings in the report by Takahashi et al. (10), newly formed acinar cells appeared and matured more slowly in the necrotic region in this study, suggesting excessive damage to the necrotic region during resection. However, similar overall results were obtained, suggesting that the regeneration of

acinar cells in the necrotic region should be observed for a prolonged time.

Takahashi et al. (9) reported the presence of many epithelial cell nests consisting of squamoid cells in granulation tissue, which formed around the necrotic region after laser irradiation. They presumed that the nests might differentiate into duct-like structures, and that striated and intercalated ducts and acini could regenerate from these duct-like structures. Hanks et al. (1) also described squamous metaplasia, which may be a tissue similar to that of squamous cell nests (9). In this study, epithelial cell nests were observed at the boundaries between atrophic and necrotic regions; these nests were adjacent to a duct-like structure with a clear lumen, as reported by Takahashi et al. (9,10), suggesting that acinar cells in the necrotic region could be regenerated from the duct-like structures.

Anti-PCNA antibodies were used to investigate cell proliferation in atrophic and necrotic regions. The results showed that cell proliferation increased in duct-like structures or duct epithelial nests on Day 7. In addition, proliferative activity was subsequently observed in newly formed acinar cells. It has been reported that the PCNA index of duct-like structures is high on day 3 in the early stage of atrophy in submandibular and sublingual glands (20,21). The previous results differed from the present findings that a few PCNA-positive cells were present in duct-like structures at the beginning of atrophy. This difference is potentially related to differences between surgical resection and ligation. In addition, the PCNA index was reportedly high at an early stage of regeneration (i.e., immediately after atrophy), but then gradually decreased; this suggests that the active proliferation of duct-like structures is not required for regeneration of acinar cells (4,21). In contrast to the previously used experimental ligation system, the present study involved a smooth transition from atrophy to regeneration; the increased cell proliferation of duct-like structures may have influenced the regeneration of newly formed acinar cells. Additionally, it is reported that the peak of proliferative activity of immature acinar cell was observed after that of duct like structure in the necrotic layer by YAG laser irradiation (9). The results of the present study were consistent with those findings. Therefore, the cell proliferation of duct-like structures is presumably involved in the regeneration of acinar cells in both the atrophic and necrotic regions.

In the present study, a round resection wound was made using a biopsy punch, and the sheet was implanted into the wound. The resection site reduced in size over time, and the mesh structure of the MedGel sheet reduced by Day 7, in conjunction with the invasion of surrounding fibrous connective tissue. The resection wound was visible on Day 10, but began to be difficult to discern on Day 14. These findings suggested that the resection wound was replaced by fibrotic connective tissue without regeneration of salivary gland tissue (2,11). It has been reported that FGF-2/ FGF receptor-1 signaling can promote atrophic rat submandibular gland repair (17). The temporospatial expression patterns of FGFs and FGF receptors were revealed in the process of rat submandibular gland regeneration (16), and it has been suggested that EGF affects the process of atrophy regeneration (14,15). However, the process of researching for the function of these growth factors is atrophy/regeneration process, and there is no paper researching for the effect on the necrotic region. In this experiment, it was

considered that the role of the physiologically active substance in the necrotic region can be examined using MedGel because the regeneration of the acinus in the necrotic region as well as the atrophic region was confirmed. Thus, this experimental model could be useful for analysis of the effects of physiologically active substances by implanting a sustained-release sheet.

## **Conclusions**

In this study, a round resection wound was prepared using a biopsy punch on the rat submandibular gland, into which a sustained-release sheet was implanted. The changes of the histology and cell proliferation during the healing process was as follows:

1. The sustained-release sheet reduced gradually in size to the one third of its original size by Day 7. The sheet disappeared almost entirely by Day 10. Three morphological regions (normal, atrophic, and necrotic) were observed around resection site.

2. In the atrophic region, acinar cells were atrophied and reduced in number, with the smallest number of acinar cells on Day 7. Beginning on Day 10, terminal acinar cells gradually regenerated. In necrotic region, on Day 7, epithelial cell nests consisting of squamoid cells appeared with duct like structure. On Day 10, newly formed acinar cells appeared, and these gradually increased until Day 21. Unlike the atrophic region, it was considered that the necrotic region did not completely regenerate.

3. The positive staining of PCNA showed the increase of proliferation activity in duct-like structures or duct epithelial nests on Day 7. Subsequent increase of proliferation activity was observed in newly formed acinar cells.

These findings could be useful when the sustained-release of growth factors is conducted using the sheet in this newly designed experimental model.

## **Acknowledgments**

I would like to express my sincere appreciation to Prof. Morio Tonogi and Associate Prof. Osamu Shimizu for their kind instruction in conducting this study.

## References

1. Hanks CT, Chaudhry AP (1971) Regeneration of rat submandibular gland following partial extirpation. A light and electron microscopic study. *Am J Anat* 130, 195-207.
2. Boshell J, Pennington C (1980) Histological observations on the effects of isoproterenol on regenerating submandibular glands of the rat. *Cell Tissue Res* 213, 411-416.
3. Kobayashi F, Matsuzaka K, Inoue T (2016) The effect of basic fibroblast growth factor on regeneration in a surgical wound model of rat submandibular glands. *Int J Oral Sci* 8, 16-23.
4. Takahashi S, Shinzato K, Nakamura S, Domon T, Yamamoto T, Wakita M (2004) Cell death and cell proliferation in the regeneration of atrophied rat submandibular glands after duct ligation. *J Oral Pathol Med* 33, 23-29.
5. Takahashi-Horiuchi Y, Sugiyama K, Sakashita H, Amano O (2008) Expression of heat shock protein 27 with the transition from proliferation to differentiation of acinar precursor cell in regenerating submandibular gland of rats. *Tohoku J Exp Med* 214, 221-230.
6. Shiratsuchi H, Shimizu O, Saito T, Mashimo T, Yonehara Y (2012) Immunohistological study of small Rho GTPases and  $\beta$ -catenin during regeneration of the rat submandibular gland. *J Mol Histol* 43, 751-759.
7. Pratt NE, Sodicoff M (1972) Ultrastructural injury following X-irradiation of rat parotid gland acinar cells. *Arch Oral Biol* 17, 1177-1186.
8. Chomette G, Auriol M, Vaillant JM, Bertrand JC, Chenal C (1981) Effects of irradiation on the submandibular gland of the rat. An enzyme histochemical and ultrastructural study. *Virchows Arch A Pathol Anat Histol* 391, 291-299.
9. Takahashi S, Wakita M (1993) Regeneration of the intralobular duct and acinus in rat submandibular glands after YAG laser irradiation. *Arch Histol Cytol* 56, 199-206.
10. Takahashi S, Wakita M (1994) Cytokeratin the intralobular glands expression duct during in rat regeneration submandibular of after YAG laser irradiation. *Arch Histol Cytol* 57, 167-173.
11. Milstein BB (1950) Regeneration in the submaxillary gland of the rat. *Br J Exp Pathol* 31, 666-669.
12. Batsakis JG (1980) Salivary gland neoplasia: an outcome of modified morphogenesis and cytodifferentiation. *Oral Surg Oral Med Oral Pathol.* 49, 229-232.
13. Takahashi S, Schoch E, Walker NI (1998) Origin of acinar cell regeneration after atrophy of the rat parotid induced by duct obstruction. *Int J Exp Pathol* 79, 293-301.
14. Takai Y, Sumitomo S, Noda Y, Asano K, Mori M (1985) Immunohistochemical observation of EGF and NGF in submandibular glands after duct ligation with or without testosterone administration. *J Oral Pathol* 14, 322-331.
15. Nagai K, Arai H, Okudera M, Yamamura T, Oki H, Komiyama K (2014) Epiregulin is critical for the acinar cell regeneration of the submandibular gland in a mouse duct ligation model. *J Oral Pathol Med* 43, 378-387.

16. Shimizu O, Yasumitsu T, Shiratsuchi H, Oka S, Watanabe T, Saito T, Yonehara Y, (2015) Immunolocalization of FGF-2, -7, -8, -10 and FGFR-1-4 during regeneration of the rat submandibular gland. *J Mol Histol* 46, 421-429.
17. Okazaki Y, Kagami H, Hattori T, Hishida S, Shigetomi T, Ueda M (2000) Acceleration of rat salivary gland tissue repair by basic fibroblast growth factor. *Arch Oral Biol* 45, 911-919.
18. Tabata Y, Nagano A, Ikada Y (1999) Biodegradation of hydrogel carrier incorporating fibroblast growth factor. *Tissue Eng* 2, 127-138.
19. Shimizu O, Shiratsuchi H, Ueda K, Oka S, Yonehara Y (2012) Alteration of the actin cytoskeleton and localisation of the  $\alpha 6\beta 1$  and  $\alpha 3$  integrins during regeneration of the rat submandibular gland. *Arch Oral Biol* 57, 1127-1132.
20. Takahashi S, Nakamura S, Suzuki R, Islam N, Domon T, Yamamoto T, Wakita M (1998) Apoptosis and mitosis of parenchymal cells in the duct-ligated rat submandibular gland. *Tissue Cell* 32, 457-463.
21. Takahashi S, Shinzato K, Nakamura S, Domon T, Yamamoto T, Wakita M (2002) The roles of apoptosis and mitosis in atrophy of the rat sublingual gland. *Tissue Cell* 34, 297-304.

## **Figures**

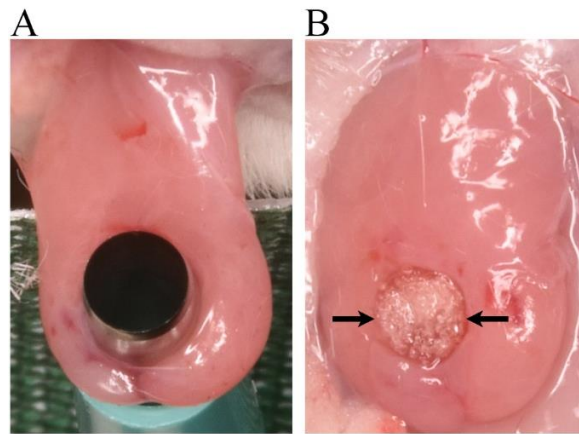


**Figure 1** Submandibular gland resection model

Submandibular gland resected by 3-mm biopsy punch (A). MedGel sheet of the same size (arrows) implanted into the resected area (B).

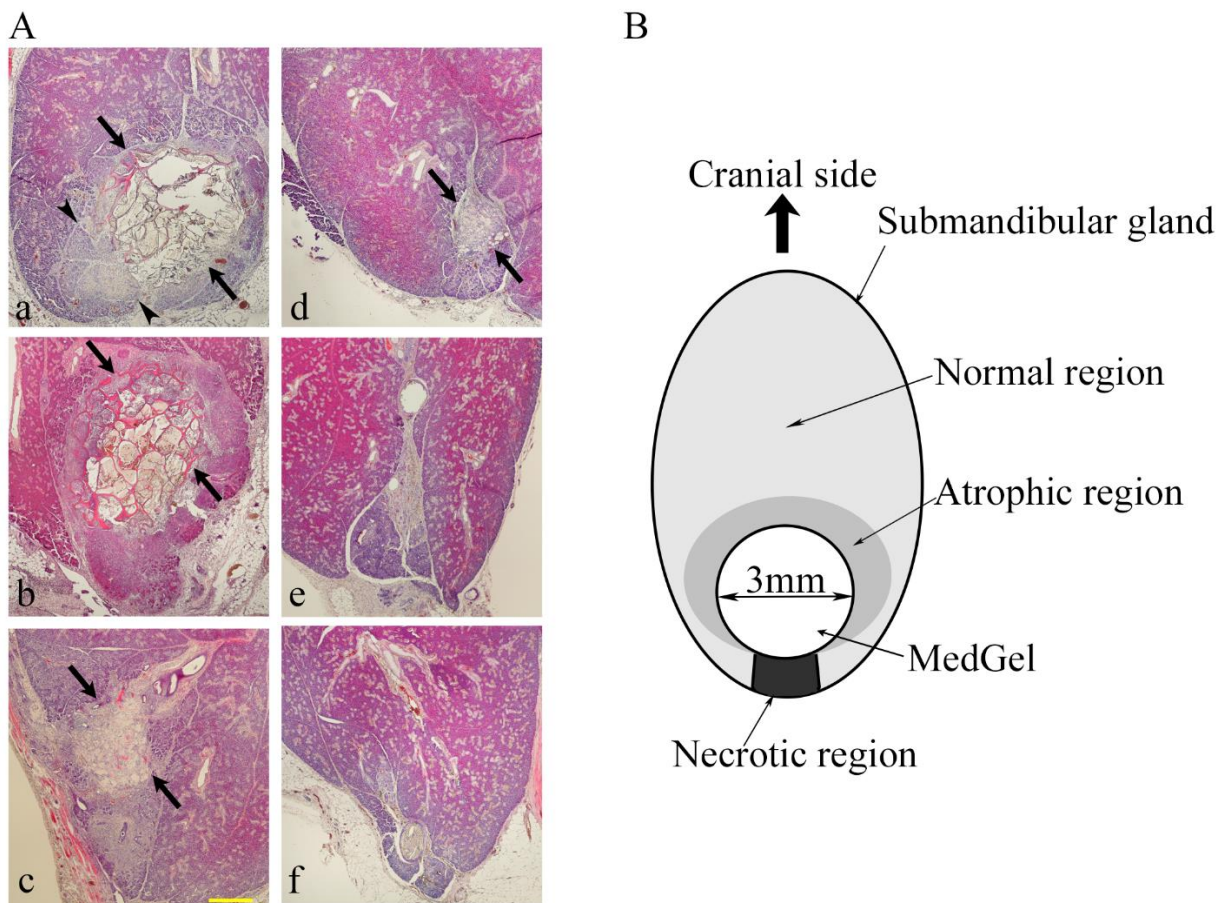


**Figure 2** HE staining images (A) of Days 3 (a), 5 (b), 7 (c), 10 (d), 14 (e), and 21 (f) after implantation of the MedGel gelatin sheet (black arrows). Note that the sheet remained for 10 days. Arrowheads indicate necrotic regions. Schematic (B) of the positional relationship in the resected area. Scale bar = 500  $\mu$ m.

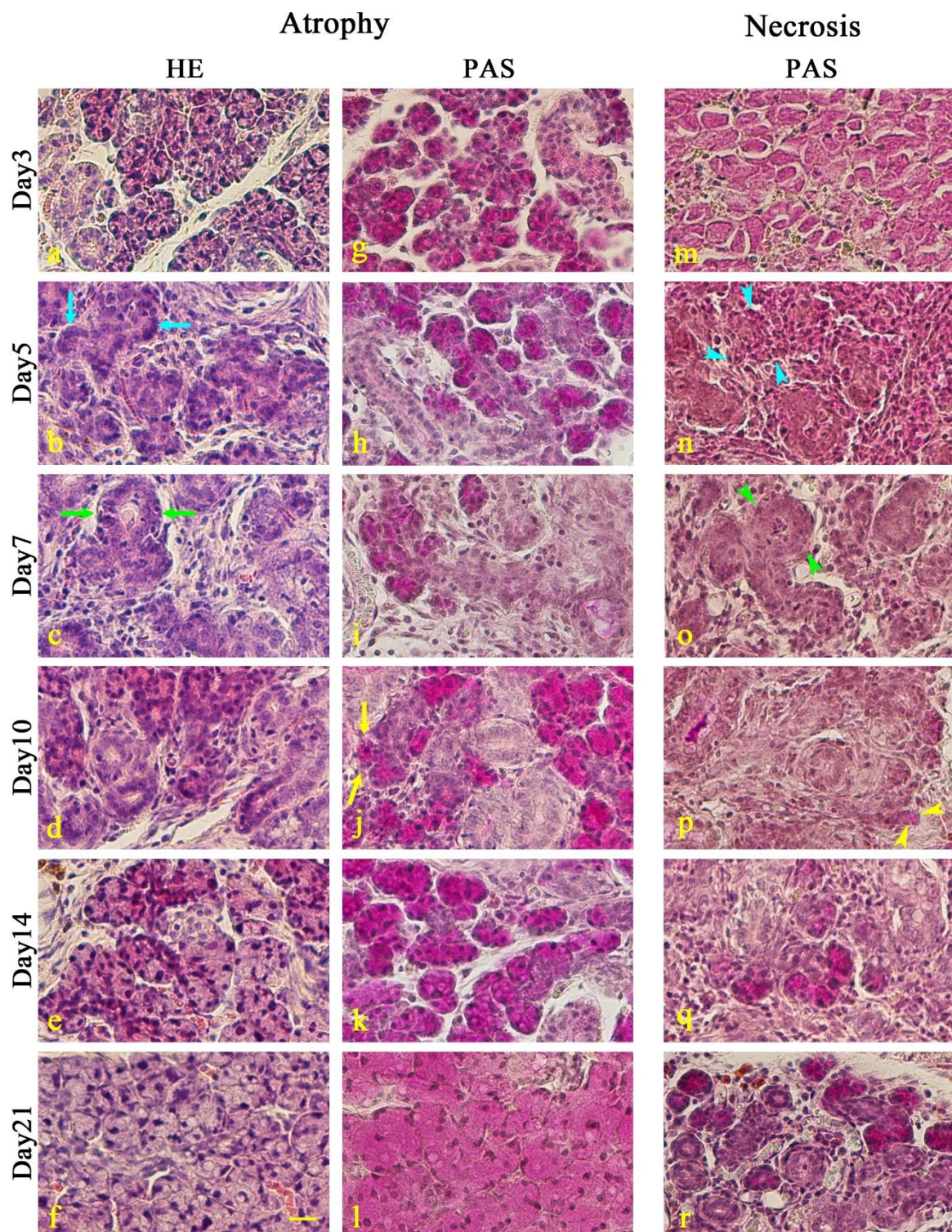


**Figure 3** HE (a-f) and PAS staining (g-r) images of atrophic (a-l) and necrotic (m-r) areas on Day 3 (a, g, m), 5 (b, h, n), 7 (c, i, o), 10 (d, j, p), 14 (e, k, q), and 21 (f, l, r). On Day 5, duct-like structures appeared in atrophic areas (blue arrows: b) and necrotic areas (blue arrowheads: n). On Day 7, epithelial nests were observed in atrophic areas (green arrows: c) and necrotic areas (green arrowheads: o). On Day 10, PAS-positive undifferentiated newly formed acinar cells (yellow arrows: j and p) were observed at the tips of duct-like structures. Scale bar = 20  $\mu$ m.

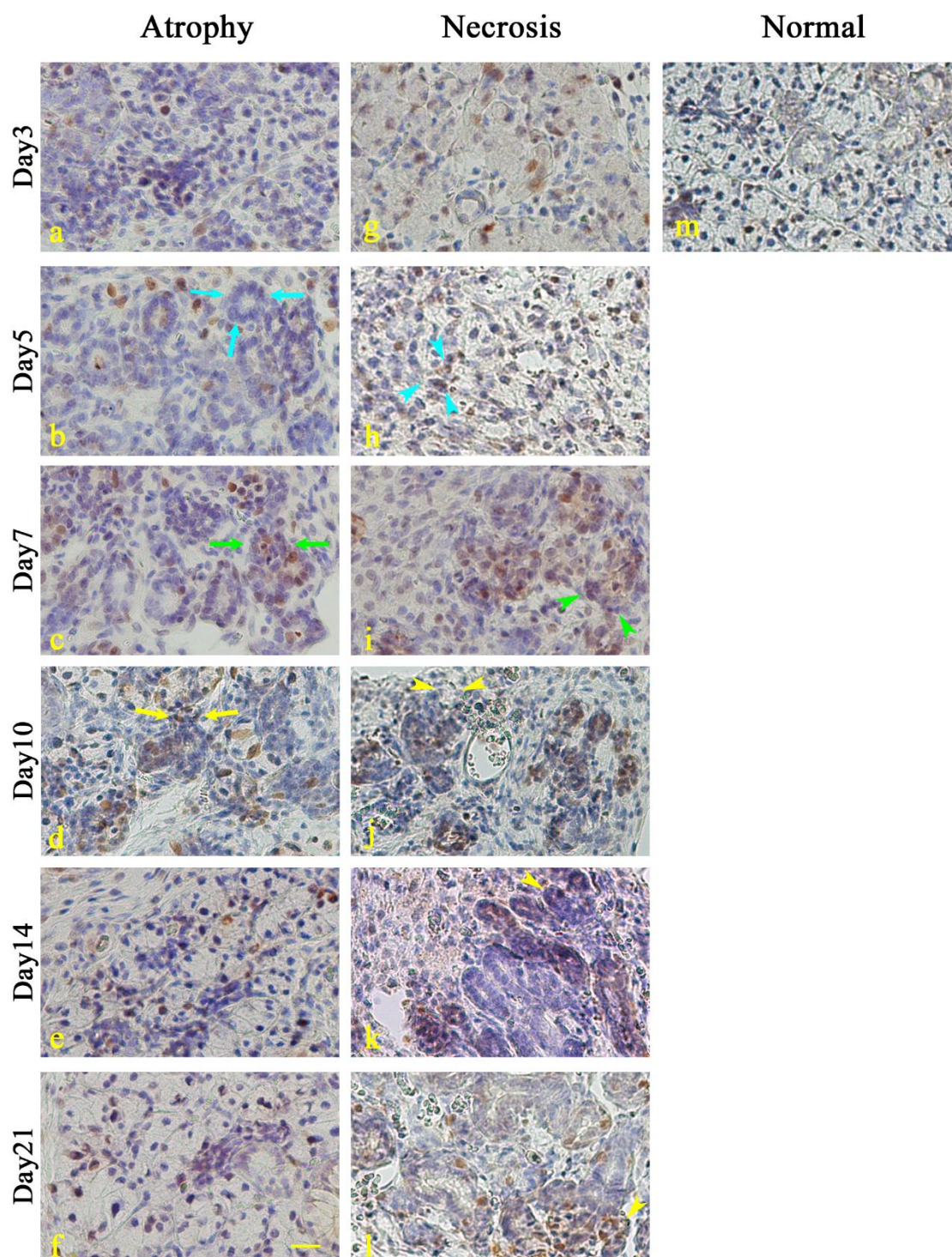


**Figure 4** Immunohistochemistry (PCNA) images of atrophic (a-f), necrotic (g-l) and normal (m) areas on Day 3 (a, g, m), 5 (b, h, n), 7 (c, i, o), 10 (d, j, p), 14 (e, k, q), and 21 (f, l, r). On Day 5, duct-like structures appeared in atrophic areas (blue arrows: b) and necrotic areas (blue arrowheads: h). On Day 7, epithelial nests were observed in atrophic areas (green arrows: c) and necrotic areas (green arrowheads: i). On Day 10-21 newly formed acinar cells in atrophic areas (yellow arrows: d) and necrotic areas (yellow arrowheads: j, k, l) were observed at the tips of duct-like structures. On Day10, PCNA of newly formed acinar cells were negative. Scale bar = 20  $\mu$ m.